The Art of Engineering Viral Nanoparticles

Jonathan K. Pokorski[†] and **Nicole F. Steinmetz**[‡,*]

[†]Department of Chemistry and The Skaggs Institute for Chemical Biology, The Scripps Research Institute, 10550 North Torrey Pines Road, La Jolla, California 92037, United States

[‡]Department of Biomedical Engineering, Case Center for Imaging Research, Case Western Reserve University, 11100 Euclid Avenue, Cleveland, Ohio 44106, United States

Abstract

Viral nanotechnology is an emerging and highly interdisciplinary field in which viral nanoparticles (VNPs) are applied in diverse areas such as electronics, energy and next-generation medical devices. VNPs have been developed as candidates for novel materials, and are often described as "programmable" because they can be modified and functionalized using a number of techniques. In this review, we discuss the concepts and methods that allow VNPs to be engineered, including (i) bioconjugation chemistries, (ii) encapsulation techniques, (iii) mineralization strategies, and (iv) film and hydrogel development. With all these techniques in hand, the potential applications of VNPs are limited only by the imagination.

Keywords

Viral nanoparticles; virus-like particles; bioconjugation; encapsulation; mineralization; hydrogels; tissue engineering

1. Viral Nanoparticles: From Pathogens to Nanomaterials

Viruses are infectious pathogens that are ubiquitous in nature. Viral diseases have been studied for more than 100 years, beginning with the discovery of the plant pathogen *Tobacco mosaic virus*,[1] and more than 5000 viruses are known to exist today. More recently, a transition has occurred. Scientists from various disciplines have discovered that viruses can be useful tools for numerous applications. In the 1950s, bacteriophages were developed as cloning vectors, as expression platforms, and as the basis for bacteriophage therapy.[2,3] Starting in the 1970s, efforts focused on the production of virus-like particles (VLPs) as vaccines against viral diseases.[4–6] A VLP is a particle composed of the virus capsid but lacking the genome, making them replication-deficient and noninfectious. (VLPs are therefore regarded as a subclass of VNPs.) For example, the *Human papilloma virus* (HPV) vaccine Gardasil is based on HPV VLPs. In the 1980s, researchers began exploiting plant viruses as expression vectors to produce pharmaceutical proteins in plants and plant cells. The advantages of expressing such proteins *in planta* using viral vectors include the absence of contamination with animal products, the low production costs and the high yields.[7–11]

Approximately 10 years ago, viruses were first defined as viral nanoparticles (VNPs). Virus structures are now regarded as nanocontainers and are used to encapsulate synthetic nanomaterials.[12] Viruses are used as scaffolds or templates to fabricate metalized

[*]Corresponding author. Mailing address: Department of Biomedical Engineering, Case Center for Imaging Research, Case Western Reserve University, 11100 Euclid Avenue, Cleveland, Ohio 44106, United States. Phone: 216 368 5590. nicole.steinmetz@case.edu.

nanoparticles and nanotube structures using mineralization techniques.[13] Attention has focused on these techniques recently, leading to the development of mineralized nanotubes and nanowires for use in batteries and data storage devices.[14–16]

Finally, bioconjugation chemistries have been combined with VNPs to enable functionalization. Early proof-of-concept studies showed that small chemical modifiers such as organic dyes and nanogold particles could be covalently attached to VNPs and that the process could be controlled with atomic precision.[17] Since then, further chemistries have been developed, ranging from standard techniques using commercially available reagents to more complex and advanced reactions. This has been fundamental in the diversification of viral nanotechnology because it allows functional components such as drugs, targeting reagents and imaging molecules to be attached to the VNP surface, allowing the development of "smart" devices for medical applications such as targeted drug-delivery and diagnostic imaging *in vivo*.

With regard to potential applications, the VNP field can be divided into several key areas: (i) the development of films and arrays for applications ranging from electronics to tissue engineering, (ii) the design of data storage and other electronic devices, (iii) the engineering of "smart" targeted devices for tissue-specific imaging and therapy, and (iv) vaccine development. In the latter case, for example, *Tomato bushy stunt virus* (TBSV) VLPs have been genetically engineered to display antigenic peptide sequences from *Human immunodeficiency virus*-1 (HIV-1), and have been shown to induce specific immune responses.[18] The use of VNPs or VLPs as vaccines has been widely reviewed.[4–6,19]

From a materials science point of view, VNPs are interesting because they can easily be produced in milligram quantities in the laboratory. The resulting particles are nanometer-sized, and are generally symmetrical, polyvalent and monodisperse. Viral capsids can be icosahedral or rod-shaped. Icosahedral particles range in size from 18 to 500 nm, whereas rod-shaped or filamentous VNPs can reach up to 2 µm in length. VNPs are exceptionally robust. The primary function of the capsid is to enclose and protect the nucleic acids, increasing their resistance to temperature and pH extremes. VNPs also remain stable in a range of solvent: buffer mixtures, which is essential for chemical modification. The VNP platforms that have been developed are summarized in Figure 1, and their pharmacological properties and applications in drug delivery and imaging have been reviewed.[20–26,27,28] The goal of this review is to highlight the methodologies and strategies used to engineer VNPs for medical applications.

2. Viral Nanoparticles in a Chemist's World: Chemical Engineering of VNPs

2.1. The Art of Bioconjugation

2.1.1. Conjugation to Natural Amino Acids—Because viral capsids are proteinaceous, standard bioconjugation protocols that address chemically reactive amino acid side chains can be used as with other proteins. The most common reactions used to modify viruses involve the reactive side chains of lysine, cysteine and aspartic/glutamic acid residues, which are accessible to *N*-hydroxysuccinimidyl (NHS) chemistry, Michael addition to maleimides, and carbodiimide activation, respectively (Figure 2A). These powerful bioconjugation chemistries have been used to attach nucleic acids, polymers and small molecules to the internal and external surfaces of viral capsids, but they are only mentioned briefly in this article because they have been reviewed extensively elsewhere.[20,21,28,29] The remainder of this section will focus on nonstandard bioconjugation methods.

One powerful new approach is the most common example of so-called "click chemistry", the copper-catalyzed azide–alkyne cycloaddition (CuAAC). The CuAAC reaction takes

place between azide and alkyne moieties in the presence of a Cu^I source and an appropriate ligand, to form a 1,4-substituted triazole (Figure 2B). The CuAAC reaction is suitable for bioconjugation because it is bioorthogonal and proceeds more quickly and with a much higher fidelity than corresponding NHS or maleimide reactions. The Finn group carried out the pioneering research on this reaction and used it to modify *Cowpea mosaic virus* (CPMV), *Hepatitis B virus* (HBV) and bacteriophage Qβ.[30–32]

The Finn group uses the CuAAC reaction when the conjugation of high-value payloads is required and a large excess of reagents is cost-prohibitive. In the following two-step protocol, high rates and yields are paramount, while bioorthogonality is not a concern. The VNP is first decorated with an azide (or an alkyne) using standard NHS chemistry to modify available lysine residues. The cargo, bearing an alkyne (or an azide, whichever has opposite functionality to the linker), is then reacted with the VNP under high-fidelity conditions in which a ligand-bound copper complex accelerates the CuAAC reaction.[33] This approach has been applied to a range of precious cargos, including sugars,[34] small molecules,[32] fullerenes[31] and proteins,[35] and these have been conjugated to both Qβ and CPMV for diverse applications ranging from vaccine development to the synthesis of novel magnetic resonance imaging (MRI) contrast agents. Recently, a highly optimized ligand-accelerated CuAAC protocol was reported, which allows the conjugation of proteins, small molecules and even notoriously fragile RNA with no degradation of the RNA species.[36] The experimental setup for successful bioconjugation using CuAAC has been described in detail.[36]

Diazonium coupling or azo coupling is bioconjugation between an activated aniline and a tyrosine side chain. The highly electron-deficient diazonium salt of *p*-nitroaniline is prepared *in situ* and directly coupled to the phenolic side chain. Coupling results in the installation of an azo linkage in the ortho position of the phenol group of the tyrosine chain (Figure 2C). Francis and co-workers have developed this coupling strategy for MS2 and TMV.[37,38] A functional group is introduced onto the VNP by activating an aniline-containing derivative of the molecule of interest to form the corresponding diazonium salt.[37] Functionalized aniline precursors, much less their diazonium salts, are generally not available commercially and must be chemically synthesized. When preparing diazo compounds, bifunctional diazonium salts can be introduced when the free end of the molecule contains a more traditional handle for bioconjugation, such as an NHS-ester or maleimide, or when the payload of interest can be attached directly to the diazo compound. Azo coupling has also been used to introduce aldehyde functionalities onto VNP scaffolds, where they serve as a target for oxime condensation reactions (Figure 2D).[37–41] The Wang group uses this type of chemistry in conjunction with CuAAC to modify surface-exposed tyrosine residues on TMV.[42] The dual methodology allows them to site-selectively label tyrosine residues with a large excess of the diazonium reagent to ensure complete conversion of all accessible residues. The subsequent use of CuAAC chemistry means that all modified side chains are labeled rapidly and with high fidelity in the presence of only modest excesses of valuable reagents.

Bioorthogonal condensation reactions between aldehyde and hydrazide groups, or aldehyde and alkoxyamine groups, are also selective and efficient. These result in hydrazone and oxime linkages, respectively, and the reactions have been adapted for VNPs based on MS2, CPMV and TMV.[37–42] In order to perform these reactions, an aldehyde is introduced onto the VNP scaffold using either an aldehyde-containing NHS derivative coupled to lysine side chains, or an aldehyde-containing diazonium salt of *p*-aniline coupled to tyrosine side chains (Figure 2D1). In the subsequent step, a hydrazide or alkoxyamine derivative of the cargo is covalently attached through the formation of a hydrazone or oxime bond (Figure 2D2). For example, polyethylene glycol (PEG) chains and chelated gadolinium complexes have been

attached to MS2 and TMV using this coupling strategy.[37–40] A high-yielding ligation approach has been developed that uses aniline as a catalyst to activate aromatic aldehydes, allowing reactions with amine nucleophiles.[43] Additionally, using hydrazone ligation strategies, CPMV VNPs have been designed that target vascular endothelial growth receptor-1, and tumor homing has been demonstrated in a preclinical mouse model.[44]

2.1.2. Bioconjugation to VNPs Using Unnatural Amino Acids—A second strategy for the modification of VNPs relies on the incorporation of unnatural amino acids into protein scaffolds. The Finn group has also pioneered efforts in this arena, in collaboration with the Tirrell group, by genetically incorporating azide or alkyne side chains into the capsids of Qβ and HBV.[30] In this approach, methionine residues are replaced with either homopropargyl glycine (HPG) or azidohomoalanine (AHA), inserting a "clickable" group in place of the natural thioether. This is done by starving a methionine-auxotroph *Escherichia coli* strain of methionine and replacing it with the desired unnatural amino acid, which then becomes incorporated in its place.[42] The method is only suitable for proteins produced in *E. coli* and those where a methionine residue can be introduced or substituted, but where these caveats do not hinder the downstream application, this is an extremely powerful tool. The unnatural amino acids AHA and HPG were incorporated into both Qβ and HBV with >95% efficiency. Once incorporated, they proved to be accessible to click protocols for the conjugation of small-molecule dyes, MRI agents, the protein transferrin, and biotin. CuAAC with these molecules resulted in nearly quantitative derivatization of the available unnatural amino acids.[30]

Another method for unnatural amino acid incorporation was developed by the Schultz group,[45] and has been implemented by Francis and co-workers to introduce an alternative bioorthogonal amino acid into MS2 for site-selective bioconjugation. The conjugation technique is regarded as an advanced conjugation chemistry, but it is useful if the modification of natural amino acids would be functionally detrimental or if the Tirrell methodology is not feasible. The approach involves the use of amber stop suppression to introduce the unnatural amino acid *p*-aminophenylalanine (pAF) into the MS2 capsid,[46] thus presenting an aniline group that allows site-selective bioconjugation at low cargo concentrations.[47] Sodium periodate-mediated oxidative coupling is used to join the unnatural amino acid to a phenylene diamine group (and later *N,N*-dimethylanisidines) containing the cargo of interest (Figure 2E). The oxidative coupling chemistry can then been used either to couple a traditional linker (such as an NHS ester or an aldehyde for oxime ligation) or to link a cargo directly to the VNP. This combined genetic and chemical methodology has been used elegantly for the site-selective addition of several molecules onto the surface of MS2, including nucleic acid aptamers, peptides and porphyrins.[46,48,49]

The marriage of molecular biology and bioconjugation chemistry is where the future development of complex VNPs lies, particularly the ability to access both natural and unnatural amino acid side chains for modification in the same VNP as this will allow the incorporation of multiple functional modalities such as targeting ligands, therapeutic moieties and imaging molecules. The examples discussed above indicate that medical applications involving multi-functionalized VNP therapeutics and imaging reagents are already on the horizon, and these are considered further in a recent review.[29]

2.2. Encapsulation of Artificial Cargos within VNPs

Viral capsids have many functions, one of which is to form a shell or tube to protect the virus genome (which can be considered a natural cargo), and another is to deliver that cargo to cells, fulfilling the virus replication cycle. Researchers developing VNPs seek to adapt the natural properties of virus coat proteins to maintain their ability to self-assemble into shells

and tubes, but at the same time to allow the encapsulation of artificial cargos such as synthetic polymers, drugs, imaging reagents, other proteins and inorganic nanoparticles.

VNPs can be purified from their natural hosts or from heterologous expression systems either as intact particles containing nucleic acids, or as VLPs that are devoid of genetic material. Several methods have been developed that allow VNPs to be disassembled into coat protein monomers *in vitro* and mixed with an artificial cargo, so that hybrid VNPs encapsulating the cargo can be reassembled (section 2.2.1). VNPs can also be exploited as constrained reaction vessels for the spatially restricted synthesis of materials inside the capsid (section 2.3). Finally, pores in the capsid structure allow small molecules to diffuse between the external medium and the capsid interior. Retention of the molecules within the capsid can be accomplished by (i) covalent attachment (section 2.1), (ii) interaction with the encapsidated nucleic acids (section 2.2.2), or (iii) trapping within the capsid by exploiting swelling mechanisms dependent on pH and metal ions (section 2.2.2).

2.2.1. Encapsulation of Materials during Particle Self-Assembly

2.2.1.1. Artificial Polymers: VNPs self-assemble naturally from coat protein monomers and encapsulate negatively charged nucleic acids, so this property can be exploited to trap artificial nucleic acids and other polyanions. When purified coat proteins are mixed with negatively charged polymers, hybrid VNPs assemble with a polymer cargo, as shown when using coat proteins from *Cowpea chlorotic mottle virus* (CCMV)[12,50] and *Hibiscus chlorotic ringspot virus* (HCRSV).[51–53] This approach has been used to encapsulate complexes of negatively charged polymers and cytotoxic drugs such as doxorubicin, allowing VNPs to be used for targeted drug-delivery (Figure 3A).[54]

2.2.1.2. Enzymes: In biological systems, enzymes are present in confined chemical microenvironments. The encapsulation of enzymes within VLPs can mimic such environments, and VNPs containing single enzyme molecules would also provide a model system to study enzymes on an individual level. The Cornellisen group has recently mixed CCMV coat proteins with the enzyme horseradish peroxidase (HRP) under stoichiometric conditions that favor the incorporation of either one HRP molecule per assembled VLP or no cargo at all.[55]

2.2.1.3. Metallic, Magnetic and Semiconductor Nanoparticles: Synthetic nanoparticles such as fluorescent quantum dots and other metallic structures are useful for imaging applications, and the encapsulation of these synthetic nanoparticles inside VNPs ensures biocompatibility, prevents aggregation, and allows the bioconjugation of functional ligands such as targeting molecules to achieve tissue-specificity. Two basic principles have been established that allow the *in vitro* self-assembly of VLPs and the encapsulation of synthetic nanoparticles: OAS-templating and polymertemplating.

OAS-templating can be achieved by decorating a nanoparticle core with a so-called origin-of-assembly site (OAS) that initiates coat protein monomer binding and promotes self-assembly. This technology was developed by the Lommel and Franzen group using *Red clover necrotic mottle virus* (RCNMV). Assembly is initiated and stabilized by an internal protein/RNA cage, which forms when a coat protein recognizes a viral RNA sequence, the OAS.[56] Artificial OAS sequences have been introduced on gold nanoparticles, magnetic nanoparticles and quantum dots, and when mixed with RCNMV coat protein monomers *in vitro*, this led to the self-assembly of RCNMV VLPs around the templated cores (Figure 3B).[57,58] Particles <17 nm in width, the interior diameter of RCNMV, were successfully encapsulated, whereas it was not possible to self-assemble VLPs around larger cores.[59]

Polymer-templating was developed by the Dragnea group using *Brome mosaic virus* (BMV). In this approach, the synthetic nanoparticle core is coated with negatively charged polymers to mimic the negative charge of the natural cargo, i.e. RNA. A range of templates have been tested, including citrate, carboxylate-terminated PEG, lipid micelles, DNA and dihydrophilic acids.[60–64] The group achieved the efficient encapsulation of gold nanoparticles, magnetic iron oxide (MIO) nanoparticles and CdSe/ZnS quantum dots into BMV VLPs using DNA and carboxylate-terminated PEG,[60,62–64] the latter yielding $95 \pm 5\%$ core-containing VLPs (Figure 3C).[60] The negative charge of the carboxylate groups mimics nucleic acids effectively, and the hydrophilic PEG polymers provide a scaffold resistant to nonspecific biomolecular interactions.

Different core particle sizes result in the formation of VLPs with different sizes and distinct symmetries. VLPs assembled from smaller nanoparticle cores are smaller than those assembled from larger gold cores.[64] A detailed analysis of BMV VLPs encapsulating different-sized gold cores by transmission electron microscopy (TEM) and 3D image reconstruction revealed that VLPs with 6 nm cores showed $T = 1$ symmetry, those with 9 nm cores resembled *pseudo T = 2* symmetry, and those with 12 nm cores showed $T = 3$ symmetry (Figure 3D). These experiments illustrate the flexibility of VNPs and their coat proteins: despite their apparent rigidity, it is clear that templating allows many different-sized hybrid structures to be assembled.

2.2.2. Infusion of Small Molecules into Assembled VNPs: Imaging Molecules and Therapeutics—Small molecules such as the lanthanide ions Gd^{3+} and Tb^{3+} can be infused into CPMV particles and trapped by making use of the encapsidated nucleic acids, e.g. 80 ± 20 Gd^{3+} and Tb^{3+} ions can be stably bound and trapped inside CPMV through interactions with RNA.[65,66] Lanthanides can also be bound at the interface of CCMV coat protein subunits by exploiting the 180 intrinsic metal ion binding sites that are present. Under physiological conditions, Ca^{2+} binds at these sites but it can be replaced with Gd^{3+} or Tb^{3+} resulting in the binding of 180 lanthanides.[67,68] Both the CPMV and CCMV particles exhibited extraordinary relaxivities *in vitro*, but because the binding affinity between Gd^{3+} and the coat proteins is low, VNPs with infused Gd^{3+} probably would not be used for *in vivo* imaging due to the risk of toxic Gd^{3+} ions diffusing in the body. From a practical point of view, a better approach would be the covalent decoration of VNPs with Gd–DOTA complexes[69] using the bioconjugation strategies discussed in section 2.1. Such VNP–lanthanide complexes would be excellent MRI contrast reagents although they have yet to be evaluated *in vivo*.

Fluorescent dyes and small molecule drugs (doxorubicin) have been infused into RCNMV particles,[70] which feature a reversible gating mechanism sensitive to pH and the concentration of metal ions. In an acidic environment the particles adopt a compact conformation, but as the pH increases a structural transition occurs causing swelling and pore-opening.[59] In the latter conformation and in the presence of RNA, small positively charged molecules can diffuse freely into the interior cavity of the particles, where they form electrostatic interactions with the RNA. Lowering of the pH causes the particles to contract again, trapping the infused cargo within. This gating mechanism can also be used to trap negatively charged polymers within VNPs.[12]

The Stockley group has demonstrated that chemically modified structural elements of VNPs can also be used to encapsulate cargo molecules. For example, MS2 phages contain a translational repression (TR) operator that binds to a TR RNA stem loop. TR operator proteins can be chemically engineered allowing small drug molecules to be covalently attached. When intact MS2 particles are exposed to such TR operators, the proteins diffuse inside the VNPs and bind stably to the 90 RNA stem loops. Therapeutic molecules such as

the ricin A chain and 5-fluorouridine have been successfully incorporated into MS2 using these principles. *In vitro* studies using receptor-targeted drug-containing MS2 VLPs confirmed cell-specific drug targeting and cytotoxicity.[71,72]

2.3. Viral Scaffolds as Templates for Materials Synthesis

Biological scaffolds such as protein cages (heat shock proteins and ferritins[23,73]) and VNPs have been used for biotemplating, a process that mimics biomineralization, i.e. the formation of inorganic structures orchestrated and governed by proteins.[74] The biotemplate, here a VNP, is exposed to metallic or other inorganic precursors, and interactions with capsid amino acids result in the nucleation of material on the external or internal surface. Rod-shaped TMV particles and filamentous M13 phages have been used extensively as templates for the synthesis of semiconducting tubes and wires for potential applications in next-generation electronics such as data storage devices[75] or battery electrodes (section 2.3.1).[14–16] The potential also exists to use such mineralized structures in medical devices.

Methods that allow the metalization or mineralization of VNPs were pioneered by the Mann group, but have been advanced by the Belcher group by combining genetic engineering, biological selection and chemistry, through the development of a library of M13 mutants selective for specific materials. The Douglas and Young groups use icosahedral particles for the spatially controlled nucleation of monodisperse nanocrystals trapped inside the biological protein scaffold, which could be used in imaging applications (Section 2.3.2) with the synthetic core facilitating detection and the biological shell conferring biocompatibility and providing a scaffold for functionalization via bioconjugation (Section 2.1). VNPs with MIO cores, for example, could be used for MRI, whereas those with fluorescent cores could be used in fluorescence spectroscopy. Most of the data reported thus far concern materials synthesis and biophysical/biochemical characterization, with *in vivo* testing the next developmental step.

2.3.1. Deposition of Materials on the External and Internal Surfaces of Viral Rods and Filaments

2.3.1.1. Mineralization of the TMV Scaffold: TMV is a highly versatile scaffold because both the external surface and the 4 nm diameter interior channel can be mineralized, and spatially controlled materials synthesis can take place because each surface has a distinct amino acid composition. Under physiological conditions, the lysine/arginine-rich exterior is positively charged, whereas the aspartate/glutamate-rich lumen is negatively charged.[76]

A broad range of materials have been deposited on TMV using different methods:

- Semiconductor nanocrystals such as PbS, CdS, and iron oxide can be nucleated under benign conditions by exposure to precursor salts.[13]

- SiO_2 layers can be formed using sol–gel condensation methods.[13]

- Noble metal coatings such as gold, silver, platinum, palladium, nickel, cobalt and copper can be achieved by electroless deposition (ELD), in which the VNPs are exposed to a metalization bath containing metal ions and a reductant (Figure 4A).[77–82]

- Atomic layer deposition (ALD) has been applied to yield aluminum oxide and titanium oxide hybrid structures. In ALD the VNP is placed in an ALD chamber and dried onto a solid support, then exposed in subsequent steps to two gasphase precursors. The procedure can be repeated until the desired layer thickness is achieved.[83]

- Conventional silica mineralization strategies can also be applied using silica-coated TMV particles as a starting material. The deposition of metals such as silver, gold, palladium and platinum can be accomplished using mercaptopropyltrimethylsilanes (MPS) as heterobivalent linker molecules to bridge the silica (silane group of MPS) and the metal (sulfur group of MPS) (Figure 4B).[84]

2.3.1.2. Biotemplating Using Genetically Engineered M13 Phages: Phage display screening technologies have been used to select peptide sequences that promote the nucleation of specific inorganic materials with a high level of selectivity and control. Such peptides can be genetically engineered into M13 phages or other VNPs, and the mutants can be used to nucleate a variety of synthetic hybrid structures, most of which find potential applications in electronics. Table 1 lists these peptide sequences and the materials they select.[85–87] Heterostructures can be synthesized by incorporating several peptides into the M13 scaffold.[87] Furthermore, different peptides can be introduced into virus body and termini by engineering different coat proteins: for example, M13 constructs expressing a gold-binding peptide as a pVIII fusion (virus body) and an antistreptavidin peptide as a pIII fusion (end structures) facilitated the self-organization of gold-coated M13 particles, end-to-end or as tripods, through interactions with streptavidin-coated gold nanoparticles (Figure 4C).[88] Metalized composites can also be assembled into higher-order structures such as films and arrays.[86,89]

2.3.2. Size-Constrained Synthesis of Inorganic Materials Using Icosahedral VNPs—VNPs and other protein cages can be used as size-constrained reaction vessels to synthesize monodisperse nanoparticles protected by the protein shell. Extensive research has been carried out with CCMV particles, which as stated above undergo reversible structural transitions based on pH and metal ion concentrations. At neutral pH the particles increase 10% in size, and 2 nm pores open in the shell, allowing free molecular exchange between the cavity and the surrounding medium.[90,91] These pH-dependent structural transitions can be coupled to mineralization reactions. If precursor salts are added while the VNP is swollen, nucleation occurs on the positively charged interior surface driven by electrostatic attraction. Lowering the pH then traps these materials inside the VNP cage. Negatively charged precursor materials such as paratungstate (Figure 4D) and decavanadate,[12] titanium oxide,[92] and Prussian Blue nanoparticles[93] can be nucleated and mineralized within the CCMV without modification. Nucleation of positively charged materials is also possible if the interior surface charge is reversed by genetically replacing basic amino acids with acidic ones.[94] Using this approach, MIO nanoparticles have been synthesized using mutant CCMV cages.[95] Particles encapsulating MIO could be useful MRI contrasting reagents.

These methods can also be applied to other VNPs as long as empty scaffolds are available. Phage T7 was used as nanocontainer and could be filled with a fluorescent europium complex[96] or metallic cobalt.[97] Similarly, the Lomonossoff and Evans groups recently established that empty CPMV particles could be internally mineralized with iron oxide and cobalt.[98] A few studies have been reported in which inorganic materials have been nucleated on the external surface of icosahedral VNPs. Genetically engineered CPMV particles externally displaying 60 peptides selective for either SiO_2 or FePt have been used for the synthesis of silica and amorphous FePt nanoparticles.[99,100]

2.4. VNPs as Scaffolds for Tissue Engineering

2.4.1. Wild-Type and Chemically Modified VNPs—For many years, the design and synthesis of materials for tissue engineering was dominated by polymer chemists and materials scientists, but the advent of VNPs has brought the combined skills and expertise of molecular biologists, biochemists and cell biologists into the field. Much of the pioneering

work has been carried out by the Wang group, using both bacteriophage and plant viruses as engineering platforms. Initial research focused on the deposition of unmodified VNPs such as CPMV ontoglass surfaces by nonspecific adsorption, followed by an assessment of their ability to promote cellular growth compared to nontreated control slides.[105]

These experiments showed that CPMV biofilms significantly enhanced cellular adhesion and proliferation, and further experiments were therefore designed to see if further enhancement could be achieved by coupling relevant ligands to VNPs using a two-step conjugation process: diazonium coupling of an alkyne to TMV followed by CuAAC to introduce the RGD peptide ligand.[106] When deposited onto glass slides, TMV displaying RGD peptides was able to promote the adherence of NIH-3T3 cells more effectively than wild-type TMV or TMV derivatized with a long-chain PEG polymer. Similar work was carried out in which the plant viruses were replaced by RGD-modified M13 particles deposited onto glass surfaces using a "slow dragging" method that caused them to align along the long axis of the VNP (Figure 5).[107] When NIH-3T3 and CHO cells were deposited onto the film, they grew along the axis of VNP orientation, leaving the researchers optimistic that this approach could begeneralized for multiple cell-types and/or ligand presentation.

The above techniques have been developed to encourage the differentiation of stem cells from progenitor to adult cells, specifically in the case of osteogenesis. Glass slides coated with either the rod-shaped TMV or the icosahedral *Turnip yellow mosaic virus* (TYMV) encouraged bone marrow stromal cells (BMSCs) to undergo osteogenic differentiation at significantly enhanced rates compared to cells grown under standard conditions.[108,109] The addressable TMV platform was then used to introduce chemical cues for differentiation, to complement the natural biogenic properties of VNPs.[42] A two-step "diazo-click" reaction (diazonium coupling of alkynes followed by CuAAC) allowed TMV particles to be decorated densely with phosphate groups. The TMV-Phos biofilm attracted calcium ions onto the tissue culture surface and increased calcium uptake by BMSCs, promoting differentiation into osteoblasts as shown by the upregulation of several relevant markers including osteocalcin, osteopontin and runx2. Titanium substrates were prepared with a TMV-Phos coating and assayed in a similar manner. As expected, these surfaces also encouraged osteogenic differentiation. The results of this study were remarkable considering the chemical simplicity of the film relative to the biological outcome, suggesting that simple cues displayed on a biocompatible surface can be used to reprogram tissues.

2.4.2. Genetically Modified VNPs—The use of chemical ligands for tissue engineering can be complemented by the genetic engineering of virus coat proteins to generate VNPs displaying specific peptides. Pasqualini and co-workers first reported the incorporation of peptide-displaying M13 VNPs into self-supporting hydrogels comprising filamentous phage particles and gold nanoparticles.[110] "Soft" materials such as these have gained attention in the tissue engineering community because they are often injectable three-dimensional matrices for cellular proliferation and/or differentiation, a significant advance since most tissue engineering applications require growth in three dimensions. These materials can self-assemble and are potentially useful for minimally invasive implantation. M13 hydrogels benefit from the natural positive charge of M13 filamentous phage particles, promoting binding to negatively charged gold nanoparticles (Figure 6A). Simple titration of the nanoscale components allows the optimal concentrations and ratios to be determined for the creation of self-supporting hydrogels. The incorporation of genetically modified M13 particles displaying integrin-binding RGD peptides within the hydrogel promotes the selective uptake of RGD phage particles into cells.

This technology has been brought forward for tissue engineering purposes by incorporating nontoxic magnetic nanoparticles such as MIO within the M13 hydrogel in order to create a system of cellular levitation whereby cells can be grown in three dimensions through the application of a magnetic field (Figure 6B,C).[111] When glioblastoma cells were grown in such a matrix, the MIO particles were internalized nonspecifically or became closely associated with the plasma membranes, and when a magnetic field was applied above the cultured cells they spontaneously levitated to the air–water interface forming a spherical bolus of cells. Cells growing in the three-dimensional matrix expanded much more rapidly than controls growing on flat surfaces, and underwent exponential proliferation in contrast to the control cells where proliferation was linear. In the context of tissue engineering applications, the main benefit of this approach is that different spatial arrangements of cells could be formed simply by changing the shape or positions of the magnets. Furthermore, multiple cell types could be positioned in close proximity to each other by magnetically levitating and arranging different populations of cells.

An alternative method to program spatial orientation and differentiation in cellular environments is the oriented deposition of genetically modified filamentous phage particles onto surfaces. Filamentous phages such as M13 are particularly advantageous in this regard because they can be aligned along their long axis in ordered films, and can also display peptides that project from the surface, allowing films to be developed with densely packed, ordered, functional peptides projecting into the medium. The Lee group exploited these two properties to create a new scaffold for oriented cell-growth and differentiation (Figure 7).[112] They displayed the extensively studied RGD and IKVAV peptide sequences on the surface of M13 particles deposited in parallel arrays on solid supports, and were able to promote the directional proliferation of neural progenitor cells.[112] Further methods were developed in which a shear force was applied during the creation of RGD-M13 thin films to create highly ordered and aligned liquid crystalline coatings for tissue culture. These surfaces were shown to be excellent platforms for the control of neural progenitor cell differentiation and neurite outgrowth (Figure 8).[113] The RGD phage films enhanced cell proliferation significantly and aligned neurite outgrowth along the axis of the M13 filaments while neurite outgrowth on wild-type and RGE control particles was disordered.

The recent proliferation of articles reporting VNP-based tissue engineering emphasizes the immense promise offered by VNP biogenic materials. Tissue regeneration and engineering is still in its infancy, but it is clear that VNPs have the potential to play a significant role in its maturation. The presentation of multiple growth factors will be necessary to mimic the extracellular matrix accurately and activate stem cell differentiation, but because VNPs can be modified in many ways both chemically and genetically, such nanoscale platforms may in the future offer a unique template to control tissue differentiation. It is likely that, as the field blossoms, biocompatible VNPs will play a crucial role in the development of novel materials for tissue engineering.

3. Summary and Outlook

Viral nanotechnology is an interdisciplinary field sitting at the interface of virology, chemistry, materials science and medicine, and has therefore facilitated the extensive cross-fertilization of ideas and techniques between these disciplines. A wide variety of protocols and strategies has been developed and implemented to modify VNPs for biomedical applications. Bioconjugation chemistries allow the site-selective conjugation of ligands for tissue-targeting, medical imaging, or drug-delivery. Further methods such as encapsulation and mineralization then allow the tuning and design of VNPs so they can be tailored for any imaginable application. VNPs can self-assemble into discrete structures and can also self-

organize into films and arrays, producing VNP hydrogels that can be used in tissue engineering.

A new era in viral nanotechnology has therefore begun in which the pathogens can be modified into tailor-made nanoscale building materials. As additional chemistries and VNP platforms become available, progress in this area is limited only by the imagination. Current developments in medicine include the engineering of VNPs as diagnostics, vaccines, imaging modalities and targeted therapeutic devices. This research shows great promise, and because viral engineering methods are well understood, the field will move rapidly into the *in vivo* stage with preclinical models and clinical trials. Viral nanotechnology is an inspiring and fast-paced field, and one that holds great promise for the development of next-generation devices and therapeutics.

Acknowledgments

References

1. Zaitlin, M. The discovery of the causal agent of the tobacco mosaic disease. In: Kung, S-D.; Yang, S-F., editors. Discoveries in Plant Biology. Hong Kong: World Publishing; 1998. p. 105-110.

2. Clark JR, March JB. Bacteriophages and biotechnology: vaccines, gene therapy and antibacterials. Trends Biotechnol. 2006; 24(5):212–218. [PubMed: 16567009]

3. Marks T, Sharp R. Bacteriophages and biotechnology: a review. J. Chem. Technol. Biotechnol. 2000; 75:6–17.

4. Garcea RL, Gissmann L. Virus-like particles as vaccines and vessels for the delivery of small molecules. Curr. Opin. Biotechnol. 2004; 15(6):513–517. [PubMed: 15560977]

5. Grgacic EV, Anderson DA. Virus-like particles: passport to immune recognition. Methods. 2006; 40(1):60–65. [PubMed: 16997714]

6. Ludwig C, Wagner R. Virus-like particles—universal molecular toolboxes. Curr. Opin. Biotechnol. 2007; 18(6):537–545. [PubMed: 18083549]

7. Canizares MC, Nicholson L, Lomonossoff GP. Use of viral vectors for vaccine production in plants. Immunol. Cell Biol. 2005; 83(3):263–270. [PubMed: 15877604]

8. Scholthof HB, Scholthof BG, Jackson AO. Plant virus vectors for transient expression of foreign proteins in plants. Annu. Rev. Phytopathol. 1996; 34:229–323.

9. Awram P, Gardner RC, Forster RL, Bellamy AR. The potential of plant viral vectors and transgenic plants for subunit vaccine production. Adv. Virus Res. 2002; 58:81–124. [PubMed: 12205784]

10. Johnson J, Lin T, Lomonossoff G. Presentation of heterologous peptides on plant viruses: genetics, structure, and function. Annu. Rev. Phytopathol. 1997; 35:67–86. [PubMed: 15012515]

11. Porta C, Lomonossoff GP. Scope for using plant viruses to present epitopes from animal pathogens. Rev. Med. Virol. 1998; 8(1):25–41. [PubMed: 10398492]

12. Douglas T, Young M. Host-Guest encapsulation of materials by assembled virus protein cages. Nature. 1998; 393:152–155.

13. Shenton W, Douglas T, Young M, Stubbs G, Mann S. Inorganic-organic nanotube composites from template mineralization of tobacco mosaic virus. Adv. Mater. 1999; 11:253–265.

14. Lee YJ, Yi H, Kim WJ, Kang K, Yun DS, Strano MS, Ceder G, Belcher AM. Fabricating genetically engineered high-power lithium-ion batteries using multiple virus genes. Science. 2009; 324(5930):1051–1055. [PubMed: 19342549]

15. Nam KT, Kim DW, Yoo PJ, Chiang CY, Meethong N, Hammond PT, Chiang YM, Belcher AM. Virus-enabled synthesis and assembly of nanowires for lithium ion battery electrodes. Science. 2006; 312(5775):885–888. [PubMed: 16601154]

16. Nam KT, Wartena R, Yoo PJ, Liau FW, Lee YJ, Chiang YM, Hammond PT, Belcher AM. Stamped microbattery electrodes based on self-assembled M13 viruses. Proc. Natl. Acad. Sci. U.S.A. 2008; 105(45):17227–17231. [PubMed: 18753629]

17. Wang Q, Lin T, Tang L, Johnson JE, Finn MG. Icosahedral virus particles as addressable nanoscale building blocks. Angew. Chem., Int. Ed. 2002; 41(3):459–462.

18. Joelson T, Akerblom L, Oxelfelt P, Strandberg B, Tomenius K, Morris TJ. Presentation of a foreign peptide on the surface of tomato bushy stunt virus. J. Gen. Virol. 1997; 78(Part 6):1213–1217. [PubMed: 9191910]

19. Plummer EM, Manchester M. Viral nanoparticles and virus-like particles: platforms for contemporary vaccine design. Wiley Interdiscip. Rev.: Nanomed. Nanobiotechnol. 2010

20. Douglas T, Young M. Viruses: making friends with old foes. Science. 2006; 312(5775):873–875. [PubMed: 16690856]

21. Evans DJ. The bionanoscience of plant viruses: templates and synthons for new materials. J. Mater. Chem. 2008; 18:3746–3754.

22. Flynn CE, Lee S-W, Peelle BR, Belcher AM. Viruses as vehicles for growth, organisation and assembly of materials. Acta Mater. 2003; 51:5867–5880.

23. Klem MT, Young MJ, Douglas T. Biomimetic magnetic nanoparticles. Mater. Today. 2005:28–37.

24. Manchester M, Singh P. Virus-based nanoparticles (VNPs): platform technologies for diagnostic imaging. Adv. Drug Delivery Rev. 2006; 58(14):1505–1522.

25. Manchester, M.; Steinmetz, NF. Viruses and Nanotechnology. Vol. Vol. 327. Berlin, Heidelberg: Springer Verlag; 2009.

26. Singh R, Kostarelos K. Designer adenoviruses for nanomedicine and nanodiagnostics. Trends Biotechnol. 2009; 27(4):220–229. [PubMed: 19251331]

27. Strable E, Finn MG. Chemical modification of viruses and virus-like particles. Curr. Top. Microbiol. Immunol. 2009; 327:1–21. [PubMed: 19198568]

28. Young M, Willits D, Uchida M, Douglas T. Plant viruses as biotemplates for materials and their use in nanotechnology. Annu. Rev. Phytopathol. 2008 46.:361–384. [PubMed: 18473700]

29. Steinmetz NF. Viral nanoparticles as platforms for next-generation therapeutics and imaging devices. Nanomedicine. 2010; 6(5):634–641. [PubMed: 20433947]

30. Strable E, Prasuhn DE, Udit AK, Brown S, Link AJ, Ngo JT, Lander G, Quispe J, Potter CS, Carragher B, Tirrell DA, Finn MG. Unnatural amino acid incorporation into virus-like particles. Bioconjugate Chem. 2008; 19:866–875.

31. Steinmetz NF, Hong V, Spoerke ED, Lu P, Breitenkamp K, Finn MG, Manchester M. Buckyballs meet viral nanoparticles: candidates for biomedicine. J. Am. Chem. Soc. 2009; 131:17093–17095. [PubMed: 19904938]

32. Prasuhn DE, Yeh RM, Obenaus A, Manchester M, Finn MG. Viral MRI contrast agents: coordination of Gd by native virions and attachment of Gd complexes by azide-alkyne cycloaddition. Chem Commun. 2007:1269–1271.

33. Prasuhn DE, Singh P, Strable E, Brown S, Manchester M, Finn MG. Plasma clearance of bacteriophage Qbeta particles as a function of surface charge. J. Am. Chem. Soc. 2008; 130:1328–1334. [PubMed: 18177041]

34. Astronomo RD, Kaltgrad E, Udit AK, Wang SK, Doores KJ, Huang CY, Pantophlet R, Paulson JC, Wong CH, Finn MG, Burton DR. Defining criteria for oligomannose immunogens for HIV using icosahedral virus capsid scaffolds. Chem. Biol. 2010; 17:357–370. [PubMed: 20416507]

35. Banerjee D, Liu AP, Voss NR, Schmid SL, Finn MG. Multivalent display and receptor-mediated endocytosis of transferrin on virus-like particles. ChemBioChem. 2010; 11:1273–1279. [PubMed: 20455239]

36. Hong V, Presolski SI, Ma C, Finn MG. Analysis and optimization of copper-catalyzed azide-alkyne cycloaddition for bioconjugation. Angew. Chem., Int. Ed. 2009; 48:9879–9883.

37. Kovacs EW, Hooker JM, Romanini DW, Holder PG, Berry KE, Francis MB. Dual-surface-modified bacteriophage MS2 as an ideal scaffold for a viral capsid-based drug delivery system. Bioconjugate Chem. 2007; 18(4):1140–1147.
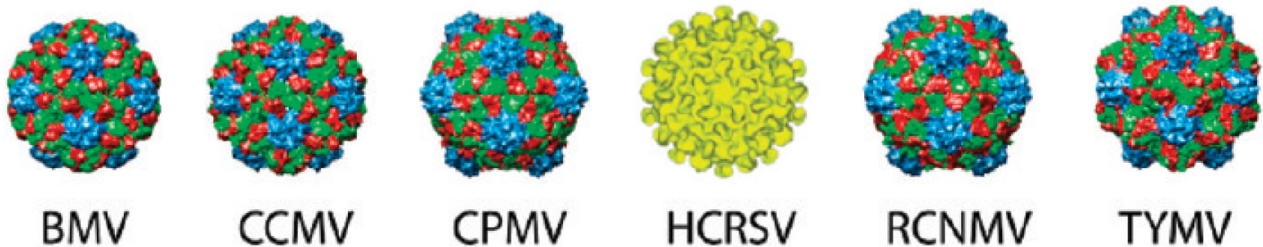
38. Schlick TL, Ding Z, Kovacs EW, Francis MB. Dual-surface modification of the tobacco mosaic virus. J. Am. Chem. Soc. 2005; 127:3718–3723. [PubMed: 15771505]

39. Datta A, Hooker JM, Botta M, Francis MB, Aime S, Raymond KN. High relaxivity gadolinium hydroxypyridonateviral capsid conjugates: nanosized MRI contrast agents. J. Am. Chem. Soc. 2008; 130(8):2546–2552. [PubMed: 18247608]

40. Hooker JM, Datta A, Botta M, Raymond KN, Francis MB. Magnetic resonance contrast agents from viral capsid shells: a comparison of exterior and interior cargo strategies. Nano Lett. 2007; 7(8):2207–2210. [PubMed: 17630809]

41. Hooker JM, O'Neil JP, Romanini DW, Taylor SE, Francis MB. Genome-free viral capsids as carriers for positron emission tomography radiolabels. Mol. Imaging Biol. 2008; 10(4):182–191. [PubMed: 18437498]

42. Kaur G, Wang C, Sun J, Wang Q. The synergistic effects of multivalent ligand display and nanotopography on osteogenic differentiation of rat bone marrow stem cells. Biomaterials. 2010; 31:5813–5824. [PubMed: 20452665]

43. Dirksen A, Dawson PE. Rapid oxime and hydrazone ligations with aromatic aldehydes for biomolecular labeling. Bioconjugate Chem. 2008; 19(12):2543–2548.

44. Brunel FM, Lewis JD, Destito G, Steinmetz NF, Manchester M, Stuhlmann H, Dawson PE. Hydrazone ligation strategy to assemble multifunctional viral nanoparticles for cell imaging and tumor targeting. Nano Lett. 2010; 10:1093–1097. [PubMed: 20163184]

45. Tian F, Tsao ML, Schultz PG. A phage display system with unnatural amino acids. J. Am. Chem. Soc. 2004; 126:15962–15963. [PubMed: 15584720]

46. Carrico ZM, Romanini DW, Mehl RA, Francis MB. Oxidative coupling of peptides to a virus capsid containing unnatural amino acids. Chem. Commun. 2008:1205–1207.

47. Hooker JM, Esser-Kahn AP, Francis MB. Modification of aniline containing proteins using an oxidative coupling strategy. J. Am. Chem. Soc. 2006; 128:15558–15559. [PubMed: 17147343]

48. Tong GJ, Hsiao SC, Carrico ZM, Francis MB. Viral capsid DNA aptamer conjugates as multivalent cell-targeting vehicles. J. Am. Chem. Soc. 2009; 131:11174–11178. [PubMed: 19603808]

49. Stephanopoulos N, Carrico ZM, Francis MB. Nanoscale integration of sensitizing chromophores and porphyrins with bacteriophage MS2. Angew. Chem. 2009; 48:9498–9502. [PubMed: 19921726]

50. Sikkema FD, Comellas-Aragones M, Fokkink RG, Verduin BJ, Cornelissen JJ, Nolte RJ. Monodisperse polymer-virus hybrid nanoparticles. Org. Biomol. Chem. 2007; 5(1):54–57. [PubMed: 17164905]

51. Bancroft JB, Hiebert E, Bracker CE. The effects of various polyanions on shell formation of some spherical viruses. Virology. 1969; 39(4):924–930. [PubMed: 5358835]

52. Ren Y, Wong SM, Lim LY. In vitro-reassembled plant virus-like particles for loading of polyacids. J. Gen. Virol. 2006; 87:2749–2754. [PubMed: 16894216]

53. Hu Y, Zandi R, Anavitarte A, Knobler CM, Gelbart WM. Packaging of a polymer by a viral capsid: the interplay between polymer length and capsid size. Biophys. J. 2008; 94(4):1428–1436. [PubMed: 17981893]

54. Ren Y, Wong SM, Lim LY. Folic acid-conjugated protein cages of a plant virus: a novel delivery platform for doxorubicin. Bioconjugate Chem. 2007; 18(3):836–843.

55. Comellas-Aragones M, Engelkamp H, Claessen VI, Sommerdijk NA, Rowan AE, Christianen PC, Maan JC, Verduin BJ, Cornelissen JJ, Nolte RJ. A virus-based single-enzyme nanoreactor. Nat. Nanotechnol. 2007; 2(10):635–639. [PubMed: 18654389]

56. Sit TL, Vaewhongs AA, Lommel SA. RNA-mediated trans-activation of transcription from a viral RNA. Science. 1998; 281(5378):829–832. [PubMed: 9694655]

57. Loo L, Guenther RH, Basnayake VR, Lommel SA, Franzen S. Controlled encapsidation of gold nanoparticles by a viral protein shell. J. Am. Chem. Soc. 2006; 128(14):4502–4503. [PubMed: 16594649]

58. Loo L, Guenther RH, Lommel SA, Franzen S. Encapsidation of nanoparticles by red clover necrotic mosaic virus. J. Am. Chem. Soc. 2007; 129(36):11111–11117. [PubMed: 17705477]

59. Sherman MB, Guenther RH, Tama F, Sit TL, Brooks CL, Mikhailov AM, Orlova EV, Baker TS, Lommel SA. Removal of divalent cations induces structural transitions in *Red clover necrotic mosaic virus*, revealing a potential mechanism for RNA release. J. Virol. 2006; 80(21):10395–10406. [PubMed: 16920821]

60. Chen C, Daniel M-C, Quinkert ZT, De M, Stein B, Bowman VD, Chipman PR, Rotello VM, Kao CC, Dragnea B. Nanoparticle-templated assembly of viral protein cages. Nano Lett. 2006; 6(4):611–615. [PubMed: 16608253]

61. Dragnea B, Chen C, Kwak ES, Stein B, Kao CC. Gold nanoparticles as spectroscopic enhancers for in vitro studies on single viruses. J. Am. Chem. Soc. 2003; 125(21):6374–6375. [PubMed: 12785770]

62. Dixit SK, Goicochea NL, Daniel MC, Murali A, Bronstein L, De M, Stein B, Rotello VM, Kao CC, Dragnea B. Quantum dot encapsulation in viral capsids. Nano Lett. 2006; 6(9):1993–1999. [PubMed: 16968014]

63. Huang X, Bronstein LM, Retrum J, Dufort C, Tsvetkova I, Aniagyei S, Stein B, Stucky G, McKenna B, Remmes N, Baxter D, Kao CC, Dragnea B. Self-assembled virus-like particles with magnetic cores. Nano Lett. 2007; 7(8):2407–2416. [PubMed: 17630812]

64. Sun J, DuFort C, Daniel MC, Murali A, Chen C, Gopinath K, Stein B, De M, Rotello VM, Holzenburg A, Kao CC, Dragnea B. Core-controlled polymorphism in virus-like particles. Proc. Natl. Acad. Sci. U.S.A. 2007; 104(4):1354–1359. [PubMed: 17227841]

65. Prasuhn DE Jr, Yeh RM, Obenaus A, Manchester M, Finn MG. Viral MRI contrast agents: coordination of Gd by native virions and attachment of Gd complexes by azide-alkyne cycloaddition. Chem. Commun. 2007; (12):1269–1271.

66. Singh P, Prasuhn D, Yeh RM, Destito G, Rae CS, Osborn K, Finn MG, Manchester M. Bio-distribution, toxicity and pathology of cowpea mosaic virus nanoparticles in vivo. J. Controlled Release. 2007; 120(1–2):41–50.

67. Allen M, Bulte JW, Liepold L, Basu G, Zywicke HA, Frank JA, Young M, Douglas T. Paramagnetic viral nanoparticles as potential high-relaxivity magnetic resonance contrast agents. Magn. Reson. Med. 2005; 54(4):807–812. [PubMed: 16155869]

68. Basu G, Allen M, Willits D, Young M, Douglas T. Metal binding to cowpea chlorotic mottle virus using terbium(III) fluorescence. J. Biol. Inorg. Chem. 2003; 8(7):721–725. [PubMed: 14505076]

69. Liepold L, Anderson S, Willits D, Oltrogge L, Frank JA, Douglas T, Young M. Viral capsids as MRI contrast agents. Magn. Reson. Med. 2007; 58(5):871–879. [PubMed: 17969126]

70. Loo L, Guenther RH, Lommel SA, Franzen S. Infusion of dye molecules into Red clover necrotic mosaic virus. Chem. Commun. 2008; (1):88–90.

71. Brown WL, Mastico RA, Wu M, Heal KG, Adams CJ, Murray JB, Simpson JC, Lord JM, Taylor-Robinson AW, Stockley PG. RNA bacteriophage capsid-mediated drug delivery and epitope presentation. Intervirology. 2002; 45(4–6):371–380. [PubMed: 12602361]

72. Wu M, Brown WL, Stockley PG. Cell-specific delivery of bacteriophage-encapsidated ricin A chain. Bioconjugate Chem. 1995; 6(5):587–595.

73. Uchida M, Klem MT, Allen M, Suci P, Flenniken ML, Gillitzer E, Varpness Z, Liepold LO, Young M, Douglas T. Biological containers: Protein cages as multifunctional nanoplatforms. Adv. Mater. 2007; 19:1025–1042.

74. Bauerlein E. Biomineralization of unicellular organisms: an unusual membrane biochemistry for the production of inorganic nano- and microstructures. Angew. Chem., Int. Ed. 2003; 42(6):614–641.

75. Tseng RJ, Tsai C, Ma L, Ouyang J, Ozkan CS, Yang Y. Digital memory device based on tobacco mosaic virus conjugated with nanoparticles. Nat. Nanotechnol. 2006; 1:72–77. [PubMed: 18654145]

76. Namba K, Stubbs G. Structure of tobacco mosaic virus at 3.6 A resolution: implications for assembly. Science. 1986; 231(4744):1401–1406. [PubMed: 3952490]

77. Balci S, Bittner AM, Hahn K, Scheu C, Knez M, Kadri A, Wege C, Jeske H, Kern K. Copper nanowires within the central channel of tobacco mosaic virus pariclces. Electrochim. Acta. 2006; 51:6251–6357.
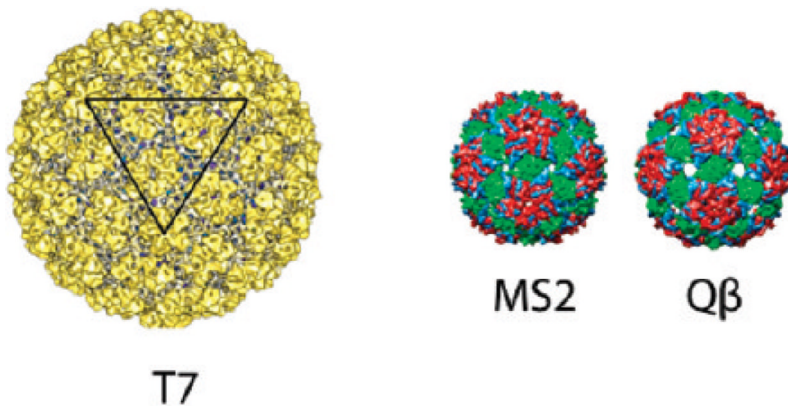
78. Dujardin E, Peet C, Stubbs G, Culver JN, Mann S. Organisation of metallic nanoparticles using Tobacco mosaic virus. Nano Lett. 2003; 3:413–417.

79. Bromley KM, Patil AJ, Perriman AW, Stubbs G, Mann S. Preparation of high quality nanowires by tobacco mosaic virus templating of gold nanoparticles. J. Mater. Chem. 2008; 18:4796–4801.

80. Knez M, Bittner AM, Boes F, Wege C, Jeske H, Maiβ E, Kern K. Biotemplate synthesis of 3-nm nickel and cobalt nanowires. Nano Lett. 2003; 3(8):1079–1082.

81. Knez M, Sumser M, Bittner AM, Wege C, Jeske H, Kooi S, Burghard M, Kern K. Electrochemical modification of individual nano-objects. J. Electroanal. Chem. 2002; 522:70–74.

82. Knez M, Sumser M, Bittner AM, Wege C, Jeske H, Martin TP, Kern K. Spatially selective nucleation of metal clusters on the tobacco mosaic virus. Adv. Funct. Mater. 2004; 14(2):116–124.

83. Knez M, Kadri A, Wege C, Gosele U, Jeske H, Nielsch K. Atomic layer deposition on biological macromolecules: metal oxide coating of tobacco mosaic virus and ferritin. Nano Lett. 2006; 6(6): 1172–1177. [PubMed: 16771575]

84. Royston ES, Brown AD, Harris MT, Culver JN. Preparation of silica stabilized Tobacco mosaic virus templates for the production of metal and layered nanoparticles. J. Colloid Interface Sci. 2009; 332(2):402–407. [PubMed: 19159894]

85. Whaley SR, English DS, Hu EL, Barbara PF, Belcher AM. Selection of peptides with semiconductor binding specificity for directed nanocrystal assembly. Nature. 2000; 405(6787): 665–668. [PubMed: 10864319]

86. Lee SW, Mao C, Flynn CE, Belcher AM. Ordering of quantum dots using genetically engineered viruses. Science. 2002; 296(5569):892–895. [PubMed: 11988570]

87. Mao C, Flynn CE, Hayhurst A, Sweeney R, Qi J, Georgiou G, Iverson B, Belcher AM. Viral assembly of oriented quantum dot nanowires. Proc. Natl. Acad. Sci. U.S.A. 2003; 100(12):6946–6951. [PubMed: 12777631]

88. Huang Y, Chiang CY, Lee SK, Gao Y, Hu EL, De Yoreo J, Belcher AM. Programmable assembly of nanoarchitectures using genetically engineered viruses. Nano Lett. 2005; 5(7):1429–1434. [PubMed: 16178252]

89. Lee SK, Yun DS, Belcher AM. Cobalt ion mediated self-assembly of genetically engineered bacteriophage for biomimetic Co-Pt hybrid material. Biomacromolecules. 2006; 7(1):14–17. [PubMed: 16398491]

90. Speir JA, Munshi S, Wang G, Baker TS, Johnson JE. Structures of the native and swollen forms of cowpea chlorotic mottle virus determined by X-ray crystallography and cryo-electron microscopy. Structure. 1995; 3(1):63–78. [PubMed: 7743132]

91. Liepold LO, Revis J, Allen M, Oltrogge L, Young M, Douglas T. Structural transitions in Cowpea chlorotic mottle virus (CCMV). Phys. Biol. 2005; 2(4):S166–S172. [PubMed: 16280622]

92. Klem MT, Young M, Douglas T. Biomimetic synthesis of β-TiO_2 inside a viral capsid. J. Mater. Chem. 2008; 18:3821–3823.

93. de la Escosura A, Verwegen M, Sikkema FD, Comellas-Aragones M, Kirilyuk A, Rasing T, Nolte RJ, Cornelissen JJ. Viral capsids as templates for the production of monodisperse Prussian blue nanoparticles. Chem. Commun. 2008; (13):1542–1544.

94. Brumfield S, Willits D, Tang L, Johnson JE, Douglas T, Young M. Heterologous expression of the modified coat protein of Cowpea chlorotic mottle bromovirus results in the assembly of protein cages with altered architectures and function. J. Gen. Virol. 2004; 85:1049–1053. [PubMed: 15039547]

95. Douglas T, Strable E, Willits D. Protein Engineering of a viral cage for constrained material synthesis. Adv. Mater. 2002; 14:415–418.

96. Liu CM, Jin Q, Sutton A, Chen L. A novel fluorescent probe: europium complex hybridized T7 phage. Bioconjugate Chem. 2005; 16(5):1054–1057.

97. Liu CM, Chung S-H, Jin Q, Sutton A, Yan F, Hoffmann A, Kay BK, Bader SD, Makowski L, Chen L. Magnetic viruses via nano-capsid templates. J. Magn. Magn. Mater. 2006; 302:47–51.

98. Aljabali AAA, Sainsbury F, Lomonossoff GP, Evans DJ. Cowpea mosaic virus unmodified empty viruslike particles loaded with metal and metal oxide. Small. 2010; 6(7):818–821. [PubMed: 20213652]

99. Shah SN, Steinmetz NF, Aljabali AAA, Lomonossoff GP, Evans DJ. Environmentally benign synthesis of virus-templated, monodisperse, iron-platinum nanoparticles. Dalton Trans. 2009; 40:8479–8480. [PubMed: 19809720]

100. Steinmetz NF, Shah SN, Barclay JE, Rallapalli G, Lomonossoff GP, Evans DJ. Virus-templated silica nanoparticles. Small. 2009; 5(7):813–816. [PubMed: 19197969]

101. Mao C, Solis DJ, Reiss BD, Kottmann ST, Sweeney RY, Hayhurst A, Georgiou G, Iverson B, Belcher AM. Virus-based toolkit for the directed synthesis of magnetic and semiconducting nanowires. Science. 2004; 303:213–217. [PubMed: 14716009]

102. Reiss BD, Mao C, Solis DJ, Ryan KS, Thomson T, Belcher AM. Biological routes to metal alloy ferromagnetic nanostructures. Nano Lett. 2004; 4(6):1127–1132.

103. Souza GR, Christianson DR, Staquicini FI, Ozawa MG, Snyder EY, Sidman RL, Miller JH, Arap W, Pasqualini R. Networks of gold nanoparticles and bacteriophage as biological sensors and cell-targeting agents. Proc. Natl. Acad. Sci. U.S.A. 2006; 103:1215–1220. [PubMed: 16434473]

104. Khalil AS, Ferrer JM, Brau RR, Kottmann ST, Noren CJ, Lang MJ, Belcher AM. Single M13 bacteriophage tethering and stretching. Proc. Natl. Acad. Sci. U.S.A. 2007; 104(12):4892–4897. [PubMed: 17360403]

105. Lin Y, Su Z, Niu Z, Li S, Kaur G, Lee LA, Wang Q. Layer-by-layer assembly of viral capsid for cell adhesion. Acta Biomater. 2008; 4(4):838–843. [PubMed: 18387348]

106. Bruckman MA, Kaur G, Lee LA, Xie F, Sepulveda J, Breitenkamp R, Zhang X, Joralemon M, Russell TP, Emrick T, Wang Q. Surface modification of tobacco mosaic virus with "click" chemistry. ChemBioChem. 2008; 9:519–523. [PubMed: 18213566]

107. Rong J, Lee LA, Li K, Harp B, Mello CM, Niu Z, Wang Q. Oriented cell growth on self-assembled bacteriophage M13 thin films. Chem. Commun. 2008:5185–5187.

108. Kaur G, Valarmathi MT, Potts JD, Wang Q. The promotion of osteoblastic differentiation of rat bone marrow stromal cells by a polyvalent plant mosaic virus. Biomaterials. 2008; 29:4074–4081. [PubMed: 18649940]

109. Kaur G, Valarmathi MT, Potts JD, Jabbari E, Sabo-Attwood T, Wang Q. Regulation of osteogenic differentiation of rat bone marrow stromal cells on 2D nanorod substrates. Biomaterials. 2010; 31:1732–1741. [PubMed: 20022632]

110. Souza GR, Christianson DR, Staquicini FI, Ozawa MG, Snyder EY, Sidman RL, Miller JH, Arap W, Pasqualini R. Networks of gold nanoparticles and bacteriophage as biological sensors and cell-targeting agents. Proc. Natl. Acad. Sci. U.S.A. 2006; 103:1215–1220. [PubMed: 16434473]

111. Souza GR, Molina JR, Raphael RM, Ozawa MG, Stark DJ, Levin CS, Bronk LF, Ananta JS, Mandelin J, Georgescu M, Bankson JA, Gelovani JG, Killian TC, Arap W, Pasqualini R. Three-dimensional tissue culture based on magnetic cell levitation. Nature Nanotechnol. 2010; 5:291–296. [PubMed: 20228788]

112. Merzlyak A, Indrakanti S, Lee S. Genetically engineered nanofiber-like viruses for tissue regenerating materials. Nano Lett. 2009; 9:846–852. [PubMed: 19140698]

113. Chung W, Merzlyak A, Yoo S, Lee S. Genetically engineered liquid-crystalline viral films for directing neural cell growth. Langmuir. 2010; 26:9885–9890. [PubMed: 20443557]

Icosahedral plant viruses

BMV   CCMV   CPMV   HCRSV   RCNMV   TYMV

Icosahedral bacteriophages

T7

MS2   Qβ

## Rod-shaped plant virus and a filamentous phage

TMV   M13
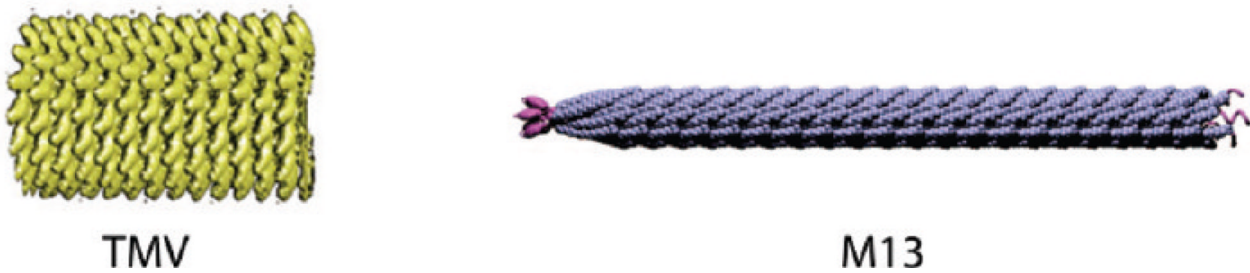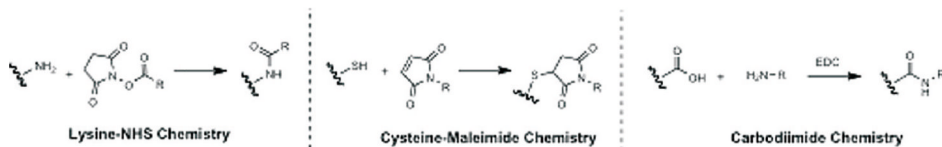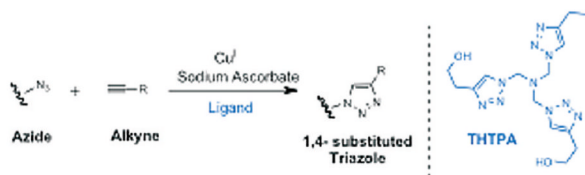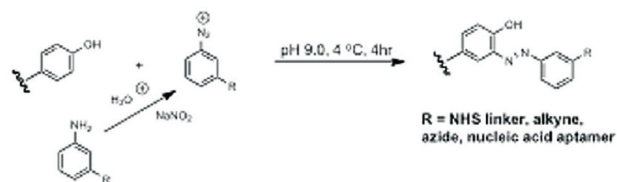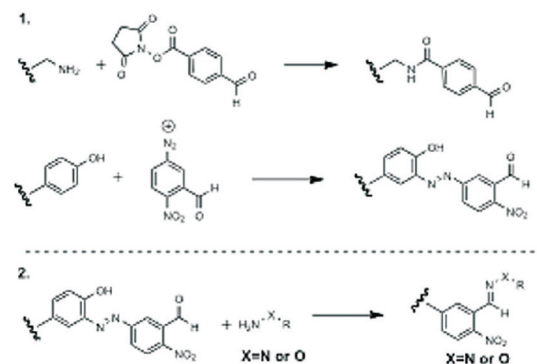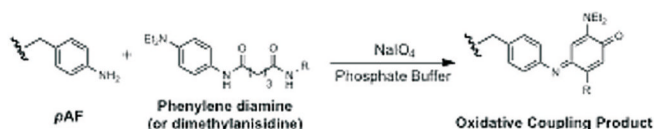
Figure 1.
An overview of the viral nanoparticles (VNPs) that have been developed for materials science and medicine. Icosahedral plant viruses: *Brome mosaic virus* (BMV), *Cowpea cholorotic mottle virus* (CCMV), *Cowpea mosaic virus* (CPMV), *Hibiscus cholorotic ringspot virus* (HCRSV), *Red clover necrotic mottle virus* (RCNMV), *Turnip yellow mosaic virus* (TYMV). Icosahedral bacteriophages: T7, MS2, and Qβ. Note that T7 is a head–tail phage, but only the head is shown. Rod-shaped and filamentous viruses: *Tobacco mosaic virus* (TMV) and phage M13. Images of the following VNPs were reproduced with permission from the VIPER database (www.viperdb.scripps.edu; Carrillo-Tripp, M.; Shepherd, C. M.; Borelli, I. A.; Venkataraman, S.; Lander, G.; Natarajan, P.; Johnson, J. E.;
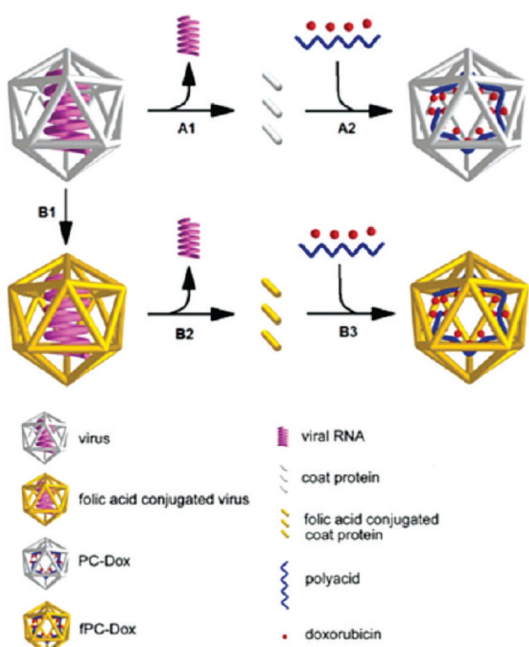
Brooks, C. L., III; Reddy, V. S. VIPERdb2: an enhanced and web API enabled relational database for structural virology. *Nucleic Acids Res.* **2009**, *37*, D436–D442. DOI: 10.1093/nar/gkn840): BMV, CCMV, CPMV, RCNMV, TYMV, MS2, Qβ. The structure of HCRSV was reproduced with permission from Doan, D. N., et al. *J. Struct. Biol.* **2003**, *144* (3), 253–261. Copyright 2003 Elsevier. The T7 structure was reproduced with permission from Agirrezabala, X., et al. *Structure* **2007**, *15*, 461–472. Copyright 2007 Elsevier. TMV was reproduced with permission from ref 28. Copyright 2008 Annual Reviews. M13 was reproduced with permission from ref 104. Copyright 2007 National Academy of Sciences.

A. Standard bioconjugation chemistries

Lysine-NHS Chemistry   Cysteine-Maleimide Chemistry   Carbodiimide Chemistry

B. Copper catalyzed azide alkyne cycloaddition (CuAAC)

Azide   Alkyne   1,4- substituted Triazole   THTPA

C. Diazonium couplings at tyrosine residues

pH 9.0, 4 °C, 4hr

R = NHS linker, alkyne, azide, nucleic acid aptamer

D. Oxime/Hydrazone ligation

1.

2.

X=N or O   X=N or O

E. Oxidative coupling to *p*-aminophenylalanine

pAF   Phenylene diamine (or dimethylanisidine)   Oxidative Coupling Product

NaIO₄ Phosphate Buffer
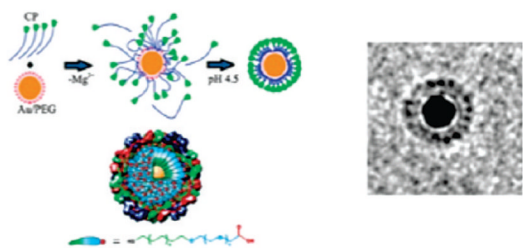
Figure 2.
Bioconjugation methods for VNPs. (A) An overview of the three most common
bioconjugation chemistries, typically addressing the most reactive amino acid residues and
often carried out using commercially available reagents. (B) The copper-catalyzed azide
alkyne cycloaddition reaction is a high-fidelity bioorthogonal reaction that can be carried out
at low reagent concentrations. (C) Diazonium coupling chemistry is a more specialized and
labor-intensive coupling process. Experienced chemists, however, should find this a
versatile method for the introduction of new functional groups onto VNPs if standard
bioconjugation protocols are inappropriate. (D) Condensation reactions to form oximes and
hydrazones. (1) Two strategies for the introduction of aldehydes into proteins. (2)

Bioorthogonal condensation reaction. (E) Oxidative coupling to the unnatural amino acid *p*-aminophenylalanine, a specific reaction that allows labeling of the unnatural amino acid in the presence of reactive side chains.
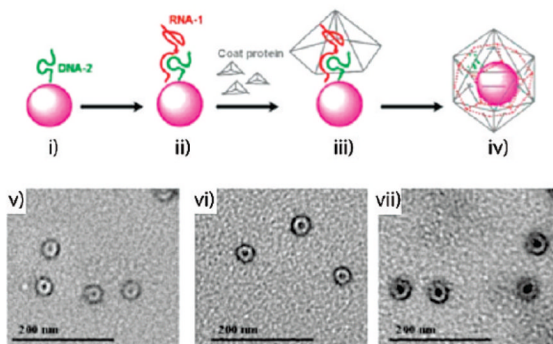
A. Artificial Polymers

C. Polymer-templated assembly


B. OAS-templated assembly

D. Size-dependence
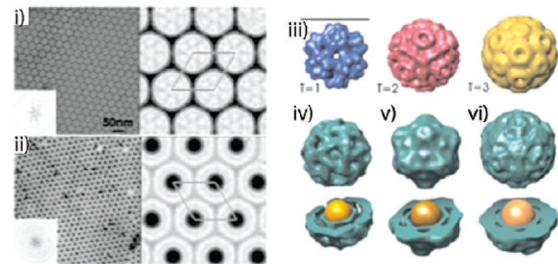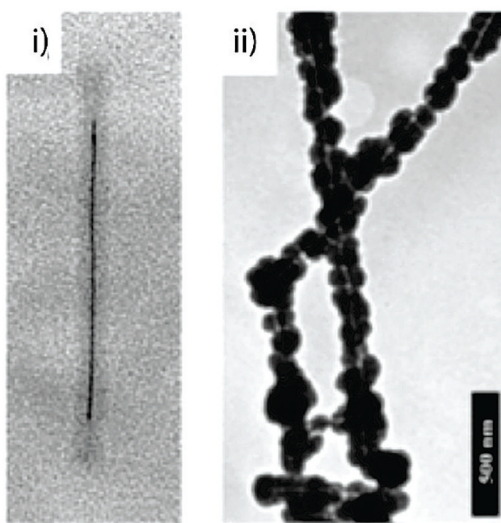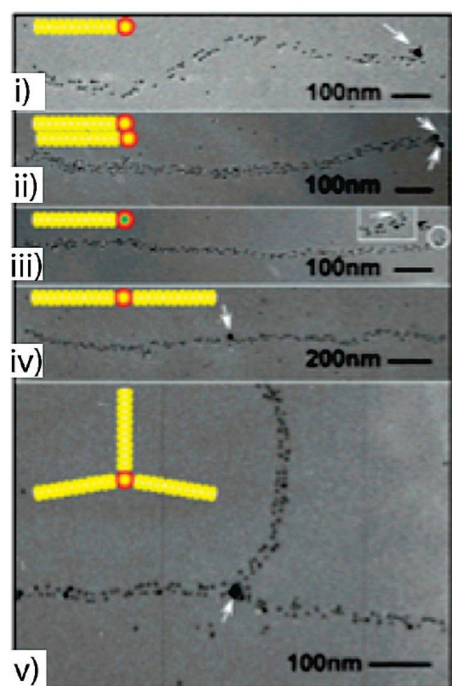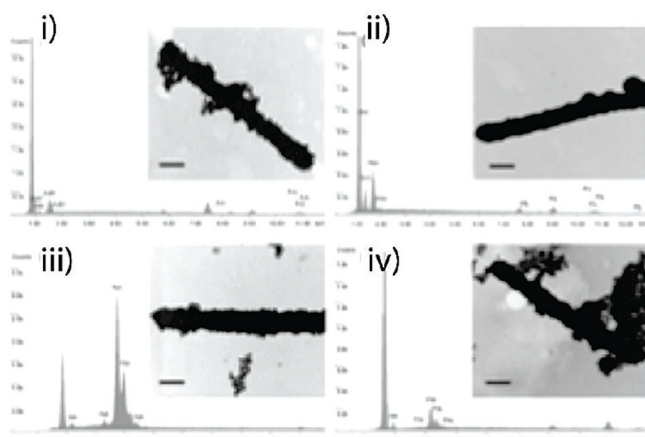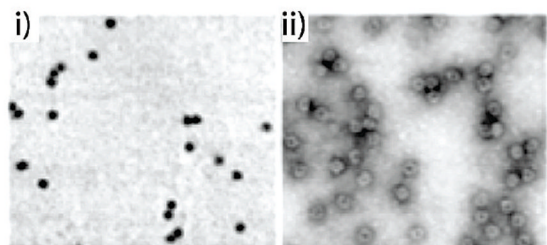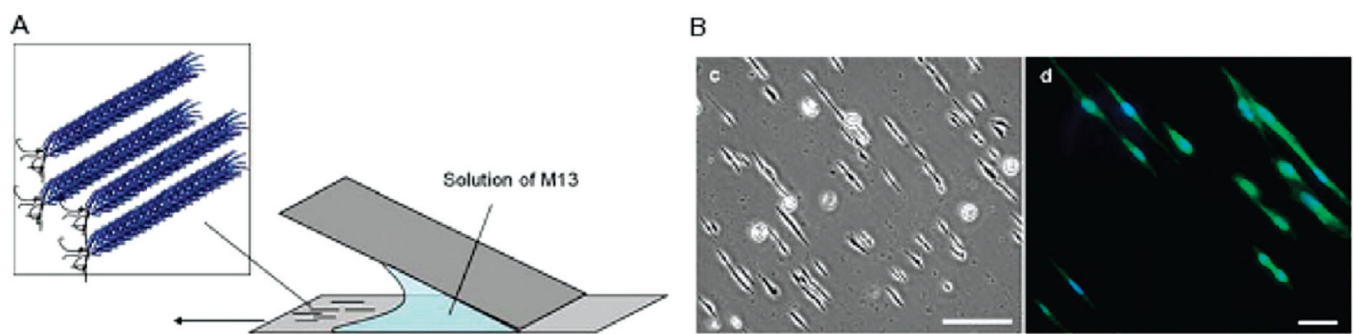
Figure 3.
(A) Artificial polymers. Schematic illustration of the preparation of a doxorubicin-loaded HCSRV protein cage with and without folic acid conjugation (fPC-Dox, PC-Dox). Steps A1 and B2 indicate the removal of viral RNA from the plant virus and purification of coat proteins. Steps A2 and B3 involve the encapsulation of polyacid and doxorubicin during the reassembly of the protein cage. Step B1 refers to the conjugation of folic acid onto the viral coat protein. Reproduced with permission from ref 54. Copyright 2007 American Chemical Society. (B) OAS-templated assembly. Top panel shows the assembly of RCNMV VLPs around a gold nanoparticles by OAS templating. (i) Conjugation of nanoparticle with DNA-2; (ii) addition of RNA-1 interacts with DNA-2 to form the functional OAS; (iii) the artificial OAS then templates the assembly of coat protein; and (iv) formation of VLP with enclosed nanoparticle. Bottom panel shows negatively stained transmission electron microscopy images of VLP encapsulating (v) 4 nm $CoFe_2O_4$, (vi) 10 nm $CoFe_2O_4$, and (vii) 15 nm $CoFe_2O_4$ nanoparticles after purification. Reproduced with permission from ref 58.

Copyright 2007 American Chemical Society. (C) Polymer-templated assembly. (i) Proposed mechanism of VLP assembly from coat proteins (CP). First, electrostatic interaction leads to the formation of disordered protein-gold nanoparticle complexes. The second step is a crystallization phase in which the protein–protein interactions lead to the formation of a regular capsid. Schematic depiction of the encapsidated nanoparticle functionalized with carboxyl-terminated tri(ethylene glycol) monomethyl ether (TEG) chains. Right panel: Cryo-electron micrograph of a single VLP. The regular arrangement of the protein structure coating the 12 nm diameter gold nanoparticle (black disk) is evident. The averages have been obtained by superposition of 10 individual images, in each case. Reproduced with permission from ref 60. Copyright 2006 American Chemical Society. (D) Size-dependence. Left panel: Negatively stained electron micrographs, Fourier transforms (insets), and corresponding Fourier projection maps. (i) BMV 2D crystal. The lattice constant is 26 nm (one unit cell is shown), and the arrangement of the densities suggests a $T = 3$ structure. (ii) VLPs containing 12 nm gold cores arranged in a 2D lattice. The lattice constant is 25 nm. Right panel: 3D reconstructions of BMV and VLP using negative stain data. (iii) $T = 1, 2,$ and 3 models of BMV capsids. The $T = 1$ and *pseudo* $T = 2$ structures were obtained from the Virus Particle ExplorR (VIPER) database. The $T = 3$ structure is the reconstructed image of BMV in this work (scale bar, 21 nm.) (iv) VLPs containing 6 nm gold cores are characterized by the absence of electron density at the 3-fold symmetry axes. The structure and diameter is close to a $T = 1$ capsid. (v) The VLPs containing 9 nm gold cores are reminiscent of a *pseudo* $T = 2$ structure. The presence of electron density at the 3-fold axes distinguishes it from the VLP structure with 6 nm cores. (vi) The shape of the VLPs containing 12 nm gold cores resembles the spherical shape of BMV although it still lacks clear evidence of hexameric capsomers. Concentric layering is a characteristic of all VLPs. Reproduced with permission from ref 64. Copyright 2007 National Academy of Sciences.
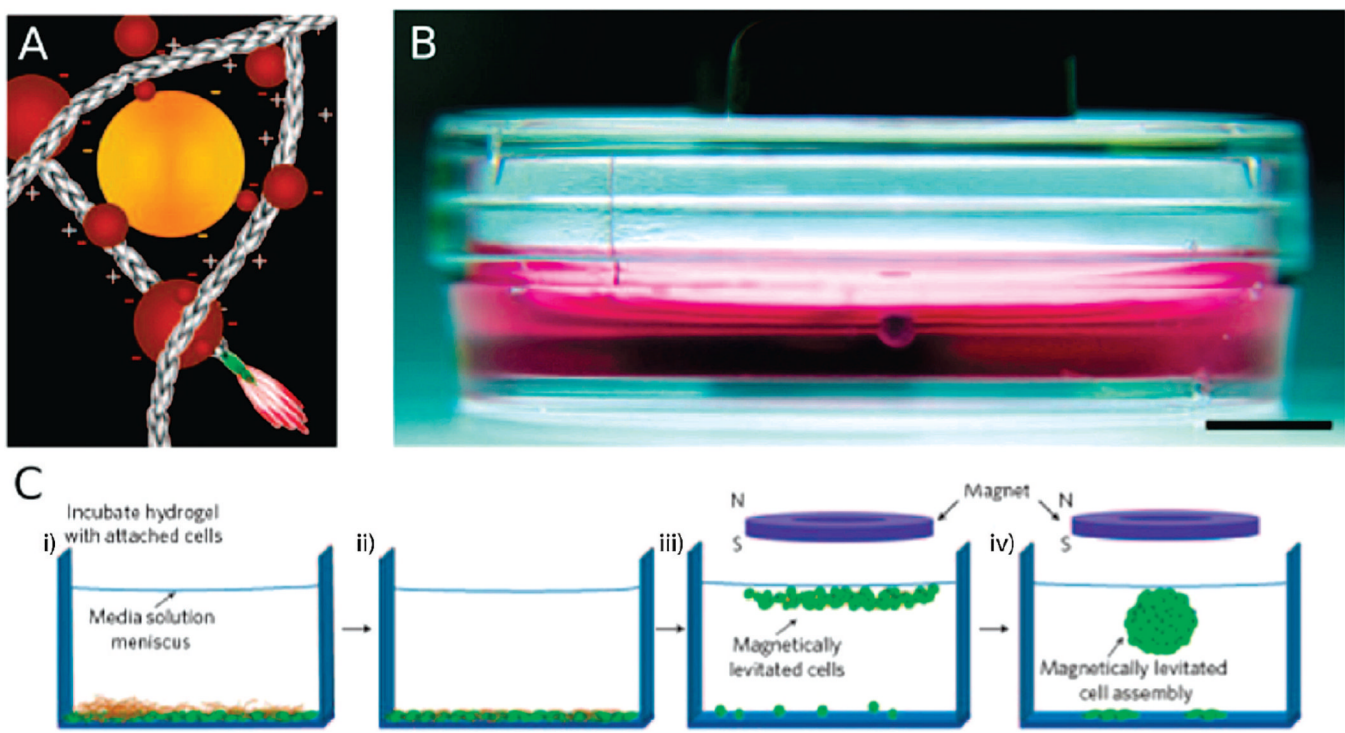
A. Electroless deposition

B. Silica-templated mineralization

C. M13 heterostructures

D. Spatial-constrained synthesis

Figure 4.
(A) Electroless deposition. Transmission electron micrographs of metalized TMV particles produced by electroless deposition. (i) TMV after Pd(II) activation, followed by electroless deposition of Ni. TMV is filled with a nickel wire with a ca. 3 nm diameter. Reproduced with permission from ref 80. Copyright 2003 American Chemical Society. (ii) TMV metalized with nickel on the external surface. Reproduced with permission from ref 82. Copyright 2004 Wiley. (B) Silica-templated mineralization. Transmission electron micrographs and accompanying energy dispersive X-ray spectra of (i) Au on thick-shell silica-coated TMV template, (ii) Ag on thick-shell silica-coated TMV template, (iii) Pt on thick-shell silica-coated TMV template, and (iv) Pd on thick-shell silica-coated TMV template. Al, Fe, and Cu peaks in the energy dispersive spectroscopy spectra are due to background effects. Scale bar = 100 nm. Reproduced with permission from 84. Copyright 2009 Elsevier. (C) M13 heterostructures. (i–v) Transmission electron micrographs of various nanoarchitectures templated by M13. Gold nanoparticles (~5 nm) bind to genetically engineered pVIII proteins along the virus axis and form 1D arrays, while a second peptide
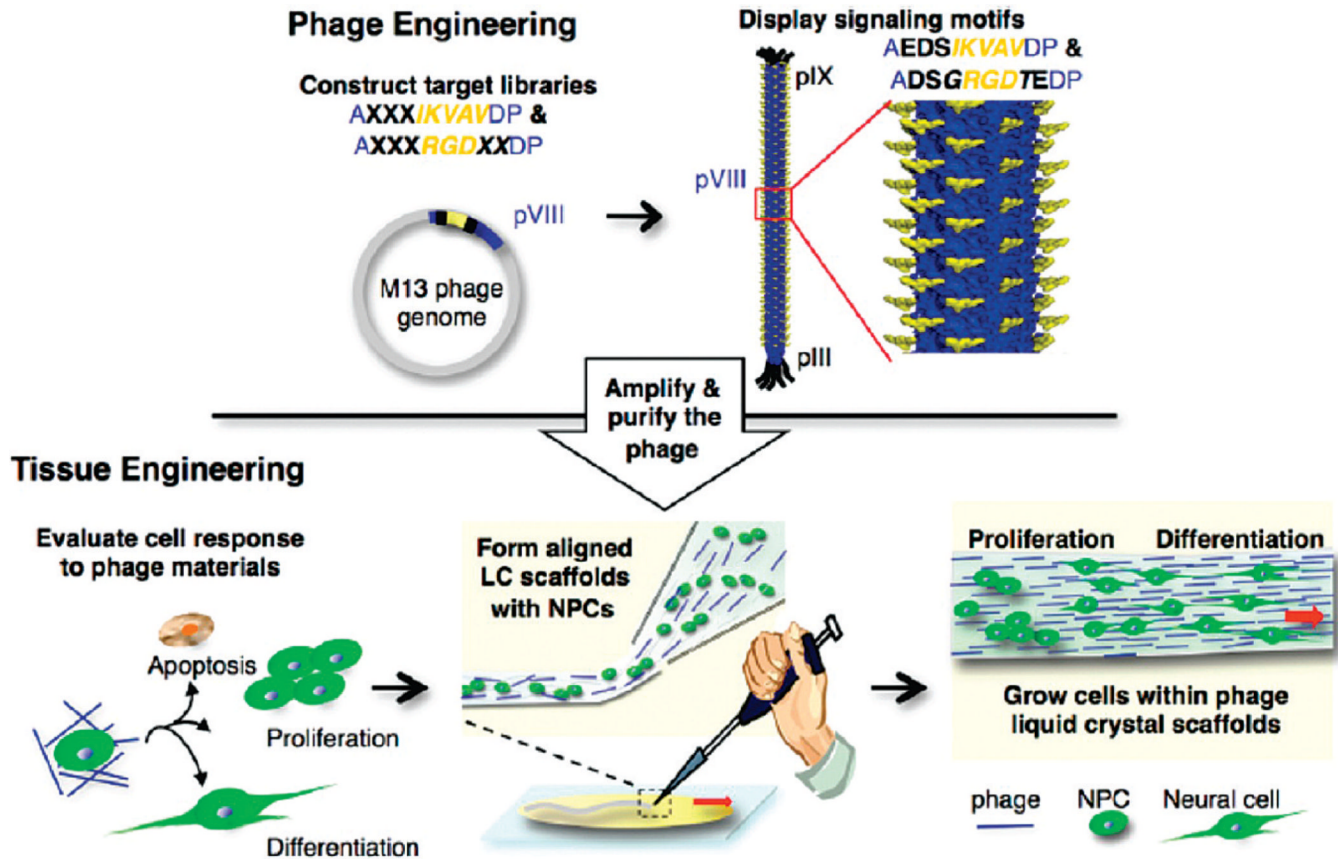
motif on pIII protein simultaneously binds to streptavidin-coated nanoparticles. Arrows highlight the streptavidin-conjugated gold nanoparticles (~15 nm) and CdSe quantum dots bound on pIII proteins. The insets show the assembly schemes of observed structures. White represents the virus structure, yellow dots represent gold nanoparticles, the green dot represents a CdSe quantum dot, and red represents the streptavidin coating around gold or CdSe particles. (C, inset) The enlarged image of the CdSe quantum dot attached to the end of the virus. Reproduced with permission from ref 88. Copyright 2005 American Chemical Society. (D) Spatially constrained synthesis. Transmission electron micrographs of paratungstate-mineralized CCMV particles after isolation by centrifugation on a sucrose gradient. (i) An unstained sample showing discrete electron dense cores; (ii) a negatively stained sample of A showing the mineral core surrounded by the intact virus protein cage. Reproduced with permission from ref 12. Copyright 1998 Nature Publishing Group.

Figure 5.
Strategy for aligned deposition of M13. (A) Aligned thin films of modified M13 particles were deposited onto glass surfaces by slowly dragging the meniscus of a high concentration solution across the surface. The shear force generated in the process caused the particles to align in the direction of the applied shear force. (B) Optical and fluorescent confocal micrographs of CHO cells cultured on aligned M13-RGD thin films. Reproduced with permission from ref 107. Copyright 2008 Royal Society of Chemistry.

Figure 6.
(A) Scheme of electrostatic interactions between magnetic iron oxide (MIO; brown spheres) and gold nanoparticles (yellow spheres) with phage (elongated structures; pIII and pVIII indicate surface capsid proteins). Nanoparticles are not drawn to scale. (B) Human glioblastoma cells (lower arrow) treated with MIO-containing hydrogel held at the air-medium interface by a magnet. The image was captured after 48 h in culture and depicts a ~1 mm spheroid. Scale bar = 5 mm. (C) (i) Hydrogel is dispersed over cells and the mixture is incubated. (ii) Washing steps remove non-interacting hydrogel fragments. Fractions of phage, gold and MIO nanoparticles enter cells or remain membrane-bound. (iii) An external magnet causes cells to rise to the air-medium interface. (iv) After 12 h of levitation, characteristic multicellular structures form (a single structure is shown here). Reproduced with permission from ref 111. Copyright 2010 Nature Publishing Group.

Figure 7.
Schematic diagram of the M13 phage tissue engineering process used by the Lee group,
showing phage engineering, cell response characterization, and the fabrication of an aligned
fiber matrix. Reproduced with permission from ref 112. Copyright 2009 American Chemical
Society.
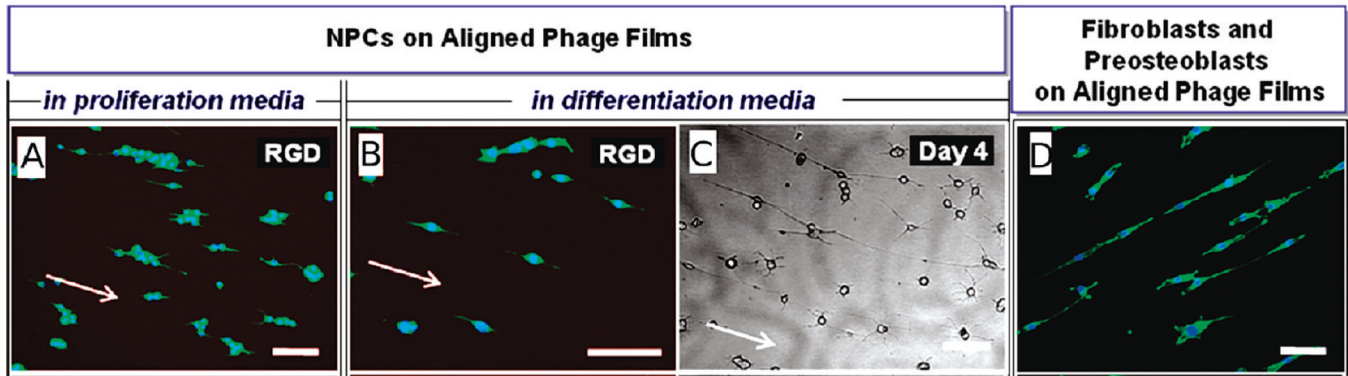
Figure 8.
Growth of neuroprogenitor cells (NPCs) and fibroblasts on aligned M13 thin films. (A)
Aligned RGD-phage film (day 1) in proliferation medium. (B) Aligned RGD-phage film
(day 1) in differentiation medium. (C) Bright-field optical micrograph of NPCs on the
aligned RGD-phage film at day 4. (D) Composite fluorescence images of NIH-3T3
fibroblasts grown on the aligned RGD-phage (12 h). Actin fibers and nuclei were stained
with phalloidin and DAPI, respectively. Scale bars = 100 µm. Reproduced with permission
from ref 113. Copyright 2010 American Chemical Society.

Table 1

Overview of the Inorganic Materials Synthesized on VNPs

material	peptide sequence (single letter code)	references
silica (SiO_2)	YSDQPTQSSQRP	100
FePt	HNKHLPSTQPLA	99, 101, 102
ZnS	CNNPMHQNC or VISNHAESSRRL	86, 87, 101
CdS	SLTPLTTSHLRS	87, 101
CoPt	CNAGDHANC	101, 102
Co^{2+}	EPGHDAVP	89
gold	VSGSSPDS	15, 88, 103, 104
silver	EEEE	16
Co_3O_4	EEEE	15, 16, 104
$FePO_4$	EEEE	14